

Search for the Decay $B_s \rightarrow \mu^+ \mu^- \phi$ in $p\bar{p}$ Collisions at $\sqrt{s} = 1.8$ TeV

D. Acosta,¹² T. Affolder,²³ H. Akimoto,⁴⁵ A. Akopian,³⁷ M. G. Albrow,¹¹ P. Amaral,⁸ D. Amidei,²⁵ K. Anikeev,²⁴ J. Antos,¹ G. Apollinari,³¹ T. Arisawa,⁴⁵ A. Artikov,⁹ T. Asakawa,⁴³ W. Ashmanskas,⁸ F. Azfar,³⁰ P. Azzi-Bacchetta,³¹ N. Bacchetta,³¹ H. Bachacou,²³ S. Bailey,¹⁶ P. de Barbaro,³⁶ A. Barbaro-Galtieri,²³ V. E. Barnes,³⁵ B. A. Barnett,¹⁹ S. Baroiant,⁵ M. Barone,¹³ G. Bauer,²⁴ F. Bedeschi,³³ S. Belforte,⁴² W. H. Bell,¹⁵ G. Bellettini,³³ J. Bellinger,⁴⁶ D. Benjamin,¹⁰ J. Bensinger,⁴ A. Beretvas,¹¹ J. P. Berge,¹¹ J. Berryhill,⁸ A. Bhatti,³⁷ M. Binkley,¹¹ D. Bisello,³¹ M. Bishai,¹¹ R. E. Blair,² C. Blocker,⁴ K. Bloom,²⁵ B. Blumenfeld,¹⁹ S. R. Blusk,³⁶ A. Bocci,³⁷ A. Bodek,³⁶ W. Bokhari,³² G. Bolla,³⁵ Y. Bonushkin,⁶ D. Bortoletto,³⁵ J. Boudreau,³⁴ A. Brandl,²⁷ S. van den Brink,¹⁹ C. Bromberg,²⁶ M. Brozovic,¹⁰ E. Brubaker,²³ N. Bruner,²⁷ E. Buckley-Geer,¹¹ J. Budagov,⁹ H. S. Budd,³⁶ K. Burkett,¹⁶ G. Busetto,³¹ A. Byon-Wagner,¹¹ K. L. Byrum,² S. Cabrera,¹⁰ P. Calafiura,²³ M. Campbell,²⁵ W. Carithers,²³ J. Carlson,²⁵ D. Carlsmith,⁴⁶ W. Caskey,⁵ A. Castro,³ D. Cauz,⁴² A. Cerri,³³ A. W. Chan,¹ P. S. Chang,¹ P. T. Chang,¹ J. Chapman,²⁵ C. Chen,³² Y. C. Chen,¹ M. -T. Cheng,¹ M. Chertok,⁵ G. Chiarelli,³³ I. Chirikov-Zorin,⁹ G. Chlachidze,⁹ F. Chlebana,¹¹ L. Christofek,¹⁸ M. L. Chu,¹ Y. S. Chung,³⁶ C. I. Ciobanu,²⁸ A. G. Clark,¹⁴ A. P. Colijn,¹¹ A. Connolly,²³ J. Conway,³⁸ M. Cordelli,¹³ J. Cranshaw,⁴⁰ R. Cropp,⁴¹ R. Culbertson,¹¹ D. Dagenhart,⁴⁴ S. D'Auria,¹⁵ F. DeJongh,¹¹ S. Dell'Agnello,¹³ M. Dell'Orso,³³ S. Demers,³⁷ L. Demortier,³⁷ M. Deninno,³ P. F. Derwent,¹¹ T. Devlin,³⁸ J. R. Dittmann,¹¹ A. Dominguez,²³ S. Donati,³³ J. Done,³⁹ M. D'Onofrio,³³ T. Dorigo,¹⁶ N. Eddy,¹⁸ K. Einsweiler,²³ J. E. Elias,¹¹ E. Engels, Jr.,³⁴ R. Erbacher,¹¹ D. Errede,¹⁸ S. Errede,¹⁸ Q. Fan,³⁶ H.-C. Fang,²³ R. G. Feild,⁴⁷ J. P. Fernandez,¹¹ C. Ferretti,³³ R. D. Field,¹² I. Fiori,³ B. Flaughner,¹¹ G. W. Foster,¹¹ M. Franklin,¹⁶ J. Freeman,¹¹ J. Friedman,²⁴ Y. Fukui,²² I. Furic,²⁴ S. Galeotti,³³ A. Gallas,^(**) M. Gallinaro,³⁷ T. Gao,³² M. Garcia-Sciveres,²³ A. F. Garfinkel,³⁵ P. Gatti,³¹ C. Gay,⁴⁷ D. W. Gerdes,²⁵ P. Giannetti,³³ P. Giromini,¹³ V. Glagolev,⁹ D. Glenzinski,¹¹ M. Gold,²⁷ J. Goldstein,¹¹ I. Gorelov,²⁷ A. T. Goshaw,¹⁰ Y. Gotra,³⁴ K. Goulianos,³⁷ C. Green,³⁵ G. Grim,⁵ P. Gris,¹¹ L. Groer,³⁸ C. Grosso-Pilcher,⁸ M. Guenther,³⁵ G. Guillian,²⁵ J. Guimaraes da Costa,¹⁶ R. M. Haas,¹² C. Haber,²³ S. R. Hahn,¹¹ C. Hall,¹⁶ T. Handa,¹⁷ R. Handler,⁴⁶ W. Hao,⁴⁰ F. Happacher,¹³ K. Hara,⁴³ A. D. Hardman,³⁵ R. M. Harris,¹¹ F. Hartmann,²⁰ K. Hatakeyama,³⁷ J. Hauser,⁶ J. Heinrich,³² A. Heiss,²⁰ M. Herndon,¹⁹ C. Hill,⁵ A. Hocker,³⁶ K. D. Hoffman,³⁵ C. Holck,³² R. Hollebeek,³² L. Holloway,¹⁸ B. T. Huffman,¹⁸ B. T. Hughes,²⁸ J. Huston,²⁶ J. Huth,¹⁶ H. Ikeda,⁴³ J. Incandela,^(***) G. Introzzi,³³ A. Ivanov,³⁶ J. Iwai,⁴⁵ Y. Iwata,¹⁷ E. James,²⁵ M. Jones,³² U. Joshi,¹¹ H. Kambara,¹⁴ T. Kamon,³⁹ T. Kaneko,⁴³ K. Karr,⁴⁴ S. Kartal,¹¹ H. Kasha,⁴⁷ Y. Kato,²⁹ T. A. Keaffaber,³⁵ K. Kelley,²⁴ M. Kelly,²⁵ D. Khazins,¹⁰ T. Kikuchi,⁴³ B. Kilminster,³⁶ B. J. Kim,²¹ D. H. Kim,²¹ H. S. Kim,¹⁸ M. J. Kim,²¹ S. B. Kim,²¹ S. H. Kim,⁴³ Y. K. Kim,²³ M. Kirby,¹⁰ M. Kirk,⁴ L. Kirsch,⁴ S. Klimenko,¹² P. Koehn,²⁸ K. Kondo,⁴⁵ J. Konigsberg,¹² A. Korn,²⁴ A. Korytov,¹² E. Kovacs,² J. Kroll,³² M. Kruse,¹⁰ S. E. Kuhlmann,² K. Kurino,¹⁷ T. Kuwabara,⁴³ A. T. Laasanen,³⁵ N. Lai,⁸ S. Lami,³⁷ S. Lammel,¹¹ J. Lancaster,¹⁰ M. Lancaster,²³ R. Lander,⁵ A. Lath,³⁸ G. Latino,³³ T. LeCompte,² A. M. Lee IV,¹⁰ K. Lee,⁴⁰ S. Leone,³³ J. D. Lewis,¹¹ M. Lindgren,⁶ T. M. Liss,¹⁸ J. B. Liu,³⁶ Y. C. Liu,¹ D. O. Litvintsev,¹¹ O. Lobban,⁴⁰ N. Lockyer,³² J. Loken,³⁰ M. Loreti,³¹ D. Lucchesi,³¹ P. Lukens,¹¹ S. Lusin,⁴⁶ L. Lyons,³⁰ J. Lys,²³ R. Madrak,¹⁶ K. Maeshima,¹¹ P. Maksimovic,¹⁶ L. Malferrari,³ M. Mangano,³³ M. Mariotti,³¹ G. Martignon,³¹ A. Martin,⁴⁷ J. A. J. Matthews,²⁷ J. Mayer,⁴¹ P. Mazzanti,³ K. S. McFarland,³⁶ P. McIntyre,³⁹ E. McKigney,³² M. Menguzzato,³¹ A. Menzione,³³ P. Merkel,¹¹ C. Mesropian,³⁷ A. Meyer,¹¹ T. Miao,¹¹ R. Miller,²⁶ J. S. Miller,²⁵ H. Minato,⁴³ S. Miscetti,¹³ M. Mishina,²² G. Mitselmakher,¹² Y. Miyazaki,²⁹ N. Moggi,³ E. Moore,²⁷ R. Moore,²⁵ Y. Morita,²² T. Moulak,³⁵ M. Mulhearn,²⁴ A. Mukherjee,¹¹ T. Muller,²⁰ A. Munar,³³ P. Murat,¹¹ S. Murgia,²⁶ J. Nachtman,⁶ V. Nagaslaev,⁴⁰ S. Nahn,⁴⁷ H. Nakada,⁴³ I. Nakano,¹⁷ C. Nelson,¹¹ T. Nelson,¹¹ C. Neu,²⁸ D. Neuberger,²⁰ C. Newman-Holmes,¹¹ C.-Y. P. Ngan,²⁴ H. Niu,⁴ L. Nodulman,² A. Nomerotski,¹² S. H. Oh,¹⁰ Y. D. Oh,²¹ T. Ohmoto,¹⁷ T. Ohsugi,¹⁷ R. Oishi,⁴³ T. Okusawa,²⁹ J. Olsen,⁴⁶ W. Orejudos,²³ C. Pagliarone,³³ F. Palmonari,³³ R. Paoletti,³³ V. Papadimitriou,⁴⁰ D. Partos,⁴ J. Patrick,¹¹ G. Pauletta,⁴² M. Paulini,^(*) C. Paus,²⁴ D. Pellett,⁵ L. Pescara,³¹ T. J. Phillips,¹⁰ G. Piacentino,³³ K. T. Pitts,¹⁸ A. Pompos,³⁵ L. Pondrom,⁴⁶ G. Pope,³⁴ M. Popovic,⁴¹ F. Prokoshin,⁹ J. Proudfoot,² F. Ptohos,¹³ O. Pukhov,⁹ G. Punzi,³³ A. Rakitine,²⁴ F. Ratnikov,³⁸ D. Reher,²³ A. Reichold,³⁰ P. Renton,³⁰ A. Ribon,³¹ W. Riegler,¹⁶ F. Rimondi,³ L. Ristori,³³ M. Riveline,⁴¹ W. J. Robertson,¹⁰ A. Robinson,⁴¹ T. Rodrigo,⁷ S. Rolli,⁴⁴ L. Rosenson,²⁴ R. Roser,¹¹ R. Rossin,³¹ C. Rott,³⁵ A. Roy,³⁵ A. Ruiz,⁷ A. Safonov,⁵ R. St. Denis,¹⁵ W. K. Sakumoto,³⁶ D. Saltzberg,⁶ C. Sanchez,²⁸ A. Sansoni,¹³ L. Santi,⁴² H. Sato,⁴³ P. Savard,⁴¹ P. Schlabach,¹¹ E. E. Schmidt,¹¹ M. P. Schmidt,⁴⁷ M. Schmitt,^(**) L. Scodellaro,³¹ A. Scott,⁶ A. Scribano,³³ S. Segler,¹¹ S. Seidel,²⁷ Y. Seiya,⁴³ A. Semenov,⁹ F. Semeria,³ T. Shah,²⁴ M. D. Shapiro,²³ P. F. Shepard,³⁴ T. Shibayama,⁴³ M. Shimojima,⁴³ M. Shochet,⁸ A. Sidoti,³¹ J. Siegrist,²³ A. Sill,⁴⁰ P. Sinervo,⁴¹ P. Singh,¹⁸ A. J. Slaughter,⁴⁷ K. Sliwa,⁴⁴ C. Smith,¹⁹

F. D. Snider,¹¹ A. Solodsky,³⁷ J. Spalding,¹¹ T. Speer,¹⁴ P. Sphicas,²⁴ F. Spinella,³³ M. Spiropulu,⁸ L. Spiegel,¹¹ J. Steele,⁴⁶ A. Stefanini,³³ J. Strologas,¹⁸ F. Strumia,¹⁴ D. Stuart,¹¹ K. Sumorok,²⁴ T. Suzuki,⁴³ T. Takano,²⁹ R. Takashima,¹⁷ K. Takikawa,⁴³ P. Tamburello,¹⁰ M. Tanaka,⁴³ B. Tannenbaum,⁶ M. Tecchio,²⁵ R. Tesarek,¹¹ P. K. Teng,¹ K. Terashi,³⁷ S. Tether,²⁴ A. S. Thompson,¹⁵ R. Thurman-Keup,² P. Tipton,³⁶ S. Tkaczyk,¹¹ D. Toback,³⁹ K. Tollefson,³⁶ A. Tollestrup,¹¹ D. Tonelli,³³ H. Toyoda,²⁹ W. Trischuk,⁴¹ J. F. de Troconiz,¹⁶ J. Tseng,²⁴ D. Tsybychev,¹¹ N. Turini,³³ F. Ukegawa,⁴³ T. Vaiciulis,³⁶ J. Valls,³⁸ S. Vejck III,¹¹ G. Velev,¹¹ G. Veramendi,²³ R. Vidal,¹¹ I. Vila,⁷ R. Vilar,⁷ I. Volobouev,²³ M. von der Mey,⁶ D. Vucinic,²⁴ R. G. Wagner,² R. L. Wagner,¹¹ N. B. Wallace,³⁸ Z. Wan,³⁸ C. Wang,¹⁰ M. J. Wang,¹ B. Ward,¹⁵ S. Waschke,¹⁵ T. Watanabe,⁴³ D. Waters,³⁰ T. Watts,³⁸ R. Webb,³⁹ H. Wenzel,²⁰ W. C. Wester III,¹¹ A. B. Wicklund,² E. Wicklund,¹¹ T. Wilkes,⁵ H. H. Williams,³² P. Wilson,¹¹ B. L. Winer,²⁸ D. Winn,²⁵ S. Wolbers,¹¹ D. Wolinski,²⁵ J. Wolinski,²⁶ S. Wolinski,²⁵ S. Worm,²⁷ X. Wu,¹⁴ J. Wyss,³³ W. Yao,²³ G. P. Yeh,¹¹ P. Yeh,¹ J. Yoh,¹¹ C. Yosef,²⁶ T. Yoshida,²⁹ I. Yu,²¹ S. Yu,³² Z. Yu,⁴⁷ A. Zanetti,⁴² F. Zetti,²³ and S. Zucchelli³

(CDF Collaboration)

¹ *Institute of Physics, Academia Sinica, Taipei, Taiwan 11529, Republic of China*

² *Argonne National Laboratory, Argonne, Illinois 60439*

³ *Istituto Nazionale di Fisica Nucleare, University of Bologna, I-40127 Bologna, Italy*

⁴ *Brandeis University, Waltham, Massachusetts 02254*

⁵ *University of California at Davis, Davis, California 95616*

⁶ *University of California at Los Angeles, Los Angeles, California 90024*

⁷ *Instituto de Fisica de Cantabria, CSIC-University of Cantabria, 39005 Santander, Spain*

⁸ *Enrico Fermi Institute, University of Chicago, Chicago, Illinois 60637*

⁹ *Joint Institute for Nuclear Research, RU-141980 Dubna, Russia*

¹⁰ *Duke University, Durham, North Carolina 27708*

¹¹ *Fermi National Accelerator Laboratory, Batavia, Illinois 60510*

¹² *University of Florida, Gainesville, Florida 32611*

¹³ *Laboratori Nazionali di Frascati, Istituto Nazionale di Fisica Nucleare, I-00044 Frascati, Italy*

¹⁴ *University of Geneva, CH-1211 Geneva 4, Switzerland*

¹⁵ *Glasgow University, Glasgow G12 8QQ, United Kingdom*

¹⁶ *Harvard University, Cambridge, Massachusetts 02138*

¹⁷ *Hiroshima University, Higashi-Hiroshima 724, Japan*

¹⁸ *University of Illinois, Urbana, Illinois 61801*

¹⁹ *The Johns Hopkins University, Baltimore, Maryland 21218*

²⁰ *Institut für Experimentelle Kernphysik, Universität Karlsruhe, 76128 Karlsruhe, Germany*

²¹ *Center for High Energy Physics: Kyungpook National University, Taegu 702-701; Seoul National University, Seoul 151-742; and SungKyunKwan University, Suwon 440-746; Korea*

²² *High Energy Accelerator Research Organization (KEK), Tsukuba, Ibaraki 305, Japan*

²³ *Ernest Orlando Lawrence Berkeley National Laboratory, Berkeley, California 94720*

²⁴ *Massachusetts Institute of Technology, Cambridge, Massachusetts 02139*

²⁵ *University of Michigan, Ann Arbor, Michigan 48109*

²⁶ *Michigan State University, East Lansing, Michigan 48824*

²⁷ *University of New Mexico, Albuquerque, New Mexico 87131*

²⁸ *The Ohio State University, Columbus, Ohio 43210*

²⁹ *Osaka City University, Osaka 588, Japan*

³⁰ *University of Oxford, Oxford OX1 3RH, United Kingdom*

³¹ *Universita di Padova, Istituto Nazionale di Fisica Nucleare, Sezione di Padova, I-35131 Padova, Italy*

³² *University of Pennsylvania, Philadelphia, Pennsylvania 19104*

³³ *Istituto Nazionale di Fisica Nucleare, University and Scuola Normale Superiore of Pisa, I-56100 Pisa, Italy*

³⁴ *University of Pittsburgh, Pittsburgh, Pennsylvania 15260*

³⁵ *Purdue University, West Lafayette, Indiana 47907*

³⁶ *University of Rochester, Rochester, New York 14627*

³⁷ *Rockefeller University, New York, New York 10021*

³⁸ *Rutgers University, Piscataway, New Jersey 08855*

³⁹ *Texas A&M University, College Station, Texas 77843*

⁴⁰ *Texas Tech University, Lubbock, Texas 79409*

⁴¹ *Institute of Particle Physics, University of Toronto, Toronto M5S 1A7, Canada*

⁴² *Istituto Nazionale di Fisica Nucleare, University of Trieste/Udine, Italy*

⁴³ *University of Tsukuba, Tsukuba, Ibaraki 305, Japan*

⁴⁴ *Tufts University, Medford, Massachusetts 02155*

⁴⁵ *Waseda University, Tokyo 169, Japan*

⁴⁶ *University of Wisconsin, Madison, Wisconsin 53706*

⁴⁷ *Yale University, New Haven, Connecticut 06520*

^(*) *Now at Carnegie Mellon University, Pittsburgh, Pennsylvania 15213*

^(**) *Now at Northwestern University, Evanston, Illinois 60208*

^(***) *Now at University of California, Santa Barbara, CA 93106*

(October 2, 2001)

We present a search for the flavor-changing neutral current decay $B_s \rightarrow \mu^+ \mu^- \phi$ in $p\bar{p}$ collisions at $\sqrt{s} = 1.8$ TeV, using 91 pb^{-1} of data collected at the Collider Detector at Fermilab (CDF). We find two candidate events for this decay, which are consistent with the background estimate of one event, and set an upper limit on the branching fraction of $\mathcal{B}(B_s \rightarrow \mu^+ \mu^- \phi) < 6.7 \cdot 10^{-5}$ at a 95% confidence level. This is the first limit on the branching fraction of this decay.

In the Standard Model of electroweak interactions, the decay $B_s \rightarrow \mu^+ \mu^- \phi$ [1] is forbidden for tree level processes. It can however proceed at low rate through higher order flavor-changing neutral current processes (FCNC), such as penguin and box diagrams. Within the Standard Model, the branching fraction is predicted to be $(1.17 \pm 0.31) \cdot 10^{-6}$ [2]. The major source of uncertainty of the prediction is due to the hadronic form factors, for which only two calculations have been published [3,4]. Observing a higher branching fraction would indicate contributions from processes beyond the Standard Model, such as, for example, Z -mediated FCNC or processes from SUSY or multi-Higgs doublet models. To date, no search for this decay has been reported. We have searched for this decay in a data sample collected during the 1992-1993 (Run 1A) and 1994-1995 (Run 1B) running periods, corresponding to a total integrated luminosity of 91 pb^{-1} .

The CDF detector configuration for Run 1 has been described in detail elsewhere [5]. The detector subsystems most relevant to this measurement are the tracking system and the muon chambers. The tracking system, which is immersed in a 1.4 T solenoidal magnetic field, consists of three detector systems. The innermost tracking device is a silicon micro-strip vertex detector (SVX) [6] which provides spatial measurements in the $r - \phi$ plane [7].

The SVX consists of two identical cylindrical barrels and has an active region of 51 cm in z ; each barrel is composed of four layers of single-sided silicon strip detectors, located at radii between 3.0 and 7.9 cm from the beam line. The impact parameter resolution of tracks measured in the SVX is $\sigma_D(p_T) = (13 + 40/p_T) \mu\text{m}$, where p_T is the transverse momentum of the track in GeV/ c . The track impact parameter D is defined as the distance of closest approach,

measured in the plane perpendicular to the beam, of the track helix to the beam axis. The SVX is followed by a set of time projection chambers (VTX) which measure the position of the proton–anti-proton interaction (the primary vertex) along the beam line. Surrounding the VTX is the Central Tracking Chamber (CTC), a 3.2 m long cylindrical drift chamber, ranging from 0.3 to 1.3 m in radius, covering the pseudorapidity interval $|\eta| < 1.1$. The CTC contains 84 layers of sense wires, grouped into nine alternating axial and stereo superlayers.

The central muon system, consisting of three components, is capable of detecting muons with $p_T \geq 1.4$ GeV/c in the pseudorapidity interval $|\eta| < 1.0$. The CMU system covers the region $|\eta| < 0.6$ and consists of four layers of planar drift chambers outside the hadron calorimeter allowing the reconstruction of track segments for charged particles penetrating the five absorption lengths of material. Outside the CMU, four layers of drift chambers are placed behind an additional three absorption lengths of steel. Finally, the CMX system extends the coverage up to pseudorapidity $|\eta| < 1.0$. Depending on the incident angle, particles have to penetrate six to nine absorption lengths of material to be detected in the CMX. For the Run 1A selection, the CMX was not used.

CDF has a three-level trigger system. The Level 1 triggers relevant for this analysis require two track segments in the muon chambers. At Level 2, tracks found in the CTC by the central fast track processor (CFT) [8] are associated to track segments in the muon chambers. Two different p_T thresholds are used in the trigger, depending on whether one or both muon track segments are required to be matched to a CFT track. When only one of the two muon track segments is associated to a CFT track, the trigger efficiency rises from 50% for tracks with $p_T = 2.6$ GeV/c to 96% for tracks with $p_T = 3.1$ GeV/c. When both muon track segments are matched to CFT tracks, the trigger efficiency rises from 50% for tracks with $p_T = 1.95$ GeV/c to 96% for tracks with $p_T = 2.3$ GeV/c. Triggers requiring two CFT track matches were not implemented during the Run 1A running period. At Level 3, both muon track segments are required to be matched to fully reconstructed CTC tracks.

In this search, the branching fraction of the decay $B_s \rightarrow \mu^+ \mu^- \phi$ is measured relative to the branching fraction of the decay $B_s \rightarrow J/\psi \phi$. With the ϕ reconstructed in the decay $\phi \rightarrow K^+ K^-$ and the J/ψ in the decay $J/\psi \rightarrow \mu^+ \mu^-$, the same final state will be observed for both decays. This similarity between the two decays allows the cancellation of most of the reconstruction and selection efficiencies, as well as of the B_s production cross-section and integrated luminosity of the data sample. In turn, the uncertainties on these factors will no longer affect the result. Differences in acceptance and trigger efficiencies nevertheless persist, and are corrected with a Monte Carlo calculation.

Candidates are reconstructed by combining two muons of opposite charge, selected by the dimuon trigger described

above, with two further tracks of opposite charge. As CDF does not possess a particle identification system suitable for this measurement, all measured tracks have to be considered as possible kaon candidates, which adds a substantial combinatorial background.

To determine whether the B_s candidate underwent a resonant or a non-resonant decay, the invariant mass of the muon pair, derived from a vertex-constrained fit of the two muons, is used. For the resonant $B_s \rightarrow J/\psi \phi$ candidates, the invariant mass of the muon pair is required to be within $80 \text{ MeV}/c^2$ of the world-average J/ψ mass, and for the non-resonant $B_s \rightarrow \mu^+ \mu^- \phi$ candidates, the invariant mass of the muon pair is required to be in the range $\mathcal{M}(\mu^+ \mu^-) < 4.4 \text{ GeV}/c^2$, with the J/ψ and $\psi(2S)$ resonances excluded in the ranges $2.9 < \mathcal{M}(\mu^+ \mu^-) < 3.3 \text{ GeV}/c^2$ and $3.6 < \mathcal{M}(\mu^+ \mu^-) < 3.8 \text{ GeV}/c^2$.

The four tracks are fitted to a common decay vertex, assigning a kaon mass to the two additional tracks and requiring the momentum vector of the B_s meson to be parallel to its flight path in the transverse ($r - \phi$) plane. In addition, for $B_s \rightarrow J/\psi \phi$ candidates, the two muons are constrained to have an invariant mass equal to the world-average J/ψ mass [9]. The confidence level of the global fit is required to be greater than 0.01 (six degrees of freedom for $B_s \rightarrow \mu^+ \mu^- \phi$ candidates and seven for $B_s \rightarrow J/\psi \phi$ candidates).

The p_T of each of the kaon tracks is required to be above $0.4 \text{ GeV}/c$ and the minimum p_T of each muon is chosen according to the trigger. For triggers requiring two CFT track matches, the p_T of both muons is required to be above $2 \text{ GeV}/c$, whereas for triggers requiring only one match, the p_T of one muon is required to be above $2.8 \text{ GeV}/c$ and the p_T of the other muon above $1.8 \text{ GeV}/c$. For data collected during Run 1A, both muons are required to have $p_T > 2 \text{ GeV}/c$.

The invariant mass of the two kaons is required to be within $\pm 10 \text{ MeV}/c^2$ of the world-average mass of the ϕ meson [9], and the p_T of the ϕ candidate is required to be above $2 \text{ GeV}/c$. The p_T of the B_s candidate is required to be above $6 \text{ GeV}/c$.

Two further requirements are imposed to reduce the background. The long lifetime of B_s mesons allows the use of the proper decay length as a strong rejection criterion against the mostly short-lived background. This requires a precise measurement of the position of the B_s meson decay (the decay vertex) and the distance the B meson traveled before decaying (the decay length). For this reason, both muons and at least one of the two kaons are required to be reconstructed in the SVX, with hits in at least three of the four layers. The proper decay length, $\lambda = L_{xy} \cdot m_{B_s} / p_T(B_s)$, is required to be above $100 \mu\text{m}$. L_{xy} is the transverse decay length, which is the distance between the $p\bar{p}$ interaction

vertex and the B_s decay vertex measured in the $r - \phi$ plane.

Due to the hard fragmentation of b quarks [10], B mesons carry most of the transverse momentum of the b -quark. A large fraction of the momentum of the tracks observed in a cone around the B meson is thus expected to be carried by the daughter tracks of the B meson. The isolation of the B_s candidate, defined as $I = p_T(B_s)/[p_T(B_s) + \sum p_T]$, is required to be greater than 0.75. The sum is the scalar sum of the transverse momenta of all the tracks, except the four tracks composing the B_s candidate, within a cone of $\Delta R \equiv \sqrt{(\Delta\eta)^2 + (\Delta\phi)^2} \leq 1$ around the momentum vector of the B_s candidate. Along the z -direction, these tracks must extrapolate to within 5 cm of the B_s candidate vertex so as to exclude tracks from other $p\bar{p}$ collisions that can occur during the same bunch crossing.

The proper decay length and isolation requirements are chosen to minimize the average upper limit that would be attained with the expected background and no true signal [9,11]. The number of background events expected in the search region is the number of events observed in the sidebands normalized to the search region. The sidebands around the B_s are chosen as the two invariant mass regions between 5.170 and 5.320 GeV/ c^2 and between 5.420 and 5.570 GeV/ c^2 . The efficiency to detect the signal is calculated using the number of $B_s \rightarrow J/\psi \phi$ candidates, which is obtained from an unbinned maximum log-likelihood fit to a Gaussian distribution above a linear background.

The signal region is chosen as a 100 MeV/ c^2 -wide invariant mass region, centered on the world-average mass of the B_s meson [9]. This is the four-track invariant mass region between 5.320 and 5.420 GeV/ c^2 . The distribution of the invariant mass of the four tracks after all selection requirements is shown in Figure 1(left) for the $B_s \rightarrow J/\psi \phi$ candidates and in Figure 1(right) for the $B_s \rightarrow \mu^+ \mu^- \phi$ candidates. While the peak observed in the resonant selection can clearly be attributed to the $B_s \rightarrow J/\psi \phi$ decay, no signal can be seen in the non-resonant selection. For the resonant selection, 11.0 ± 3.5 $B_s \rightarrow J/\psi \phi$ candidates are found, while in the non-resonant selection, two candidates are counted in the search region, with an expected background, extrapolated from the sidebands, of one event.

Finding no evidence for a signal, an upper limit on the branching fraction is set. The low number of candidate and background events does not warrant a background subtraction, and the observed candidates in the search region are assumed to be signal events. This results in Poisson upper limits of 5.32 and 6.30 events at a 90% and 95% confidence level respectively.

The upper limit on the branching fraction is given by

$$\mathcal{B}(B_s \rightarrow \mu^+ \mu^- \phi) < N_{\text{limit}}(B_s \rightarrow \mu^+ \mu^- \phi)$$

$$\times \frac{\mathcal{B}(B_s \rightarrow J/\psi \phi, J/\psi \rightarrow \mu^+ \mu^-)}{N(B_s \rightarrow J/\psi \phi) \cdot \epsilon_{\text{cut}} \cdot \epsilon_{\text{mass}} \cdot \epsilon_{\text{SD}}}.$$

The factor ϵ_{cut} contains the ratio of the acceptance and efficiencies of the two decays that do not cancel. It is calculated using a Monte Carlo simulation of both decays. The decay $B_s \rightarrow \mu^+ \mu^- \phi$ is modelled according to the prediction of the decay matrix elements [12] using the Wilson coefficients presented in Reference [13] and the hadronic form factors presented in Reference [3]. The factor ϵ_{mass} contains the extrapolation of the result from the non-resonant to the full invariant mass range and the factor ϵ_{SD} the compensation of the contribution of long-distance processes in the non-resonant mass range. These two correction factors are obtained by performing numerical integrations of the analytical expression of the differential decay width. The product of these factors is found to be $\epsilon_{\text{cut}} \cdot \epsilon_{\text{mass}} \cdot \epsilon_{\text{SD}} = (0.912 \pm 0.059)$. The uncertainty is due to variations in the trigger efficiency parameterizations and on the choice of a particular decay model. The latter is estimated by replacing the hadronic form factors used by those presented in Reference [4]. These two sets of form factors are the only two published for this decays so far. A comparison of the form factors at $q^2 \equiv \mathcal{M}^2(\mu^+ \mu^-) = 0$ shows that the two calculations agree within the estimated accuracy of the models (15%) [3].

The total systematic uncertainty on the measurement of the branching fraction is 48.0%. It is included in the upper limit of candidates with the prescription described in Reference [14]. The dominant contributions are the uncertainties on the branching fraction of the reference decay ($\mathcal{B}(B_s \rightarrow J/\psi \phi, J/\psi \rightarrow \mu^+ \mu^-) = (5.5 \pm 1.9) \cdot 10^{-5}$: 35.5% [9,15]) and the statistical uncertainty on the number of resonant candidates observed (31.8%). The uncertainty on the product of the three correction factors ($\epsilon_{\text{cut}} \cdot \epsilon_{\text{mass}} \cdot \epsilon_{\text{SD}}$) is small (6.5%).

With these results, the following 90% and 95% C.L. upper limits of the branching fraction are measured:

$$\mathcal{B}(B_s \rightarrow \mu^+ \mu^- \phi) < 4.7 \cdot 10^{-5} \text{ (90\%CL)}$$

$$\mathcal{B}(B_s \rightarrow \mu^+ \mu^- \phi) < 6.7 \cdot 10^{-5} \text{ (95\%CL)}.$$

In conclusion, we have searched for the FCNC decay $B_s \rightarrow \mu^+ \mu^- \phi$ in $p\bar{p}$ collisions at $\sqrt{s} = 1.8$ TeV using 91.4 pb⁻¹ of data. We have observed no significant signal, and set the first limit on the branching fraction of this decay.

We thank the Fermilab staff and the technical staffs of the participating institutions for their vital contributions. This work was supported by the U.S. Department of Energy and National Science Foundation; the Italian Istituto Nazionale di Fisica Nucleare; the Ministry of Education, Science and Culture of Japan; the Natural Sciences and

- [1] Charge conjugation is implied throughout this paper.
- [2] The branching fraction predicted in the Standard Model is calculated using the expression of the differential decay width presented in Reference [12], with the Wilson coefficients presented in Reference [13] and the hadronic form factors presented in Reference [3]. For the B_s mass and lifetime, $m(B_s) = 5369.6 \pm 2.4 \text{ MeV}/c^2$ and $c\tau(B_s) = 1.493 \pm 0.0062 \text{ ps}$ are used [9]. For $|V_{ts}|$, the value derived in Reference [12] ($|V_{ts}| = 0.038 \pm 0.005(\text{exp})$) is used, and $|V_{tb}| = 1$ is assumed.
- [3] D. Melikhov and B. Stech, *Phys. Rev.* **D 62**, 014006 (2000).
- [4] P. Ball and V.M. Braun, *Phys. Rev.* **D 58**, 094016 (1998).
- [5] CDF Collaboration, F. Abe *et al.*, *Nucl. Instrum. Methods* **A 271**, 387 (1988); CDF Collaboration, F. Abe *et al.*, *Phys. Rev.* **D 50**, 2966 (1994).
- [6] D. Amidei *et al.*, *Nucl. Instrum. Methods* **A 350**, 73 (1994).
- [7] The polar angle (θ) in cylindrical coordinates is measured from the proton beam which defines the z -axis, and the azimuthal angle (ϕ) from the plane of the Tevatron. The rapidity (y) is defined as $y = \tanh^{-1}(p_z/E)$. The pseudorapidity (η) is defined as $\eta = -\ln(\tan(\theta/2))$. Throughout this paper 'transverse' refers to the plane perpendicular to the proton beam and 'longitudinal' refers to the axis parallel to the proton beam (z -axis).
- [8] G. Foster *et al.*, *Nucl. Instrum. Methods* **A 269**, 93 (1988).
- [9] Particle Data Group, *Review of Particle Properties*, D.E. Groom *et al.*, *E. Phys. J.* **C 15**, 1 (2000).
- [10] C. Peterson *et al.*, *Phys. Rev.* **D 27**, 105 (1983).
- [11] G.J. Feldman and R.D. Cousins, *Phys. Rev.* **D 57**, 3873 (1998).
- [12] D. Melikhov, N. Nikitin and S. Simula, *Phys. Rev.* **D 57**, 6814 (1998).
- [13] A.J.Buras and M. Münz, *Phys. Rev.* **D 52**, 186 (1995).
- [14] R.D. Cousins and V.L. Highland, *Nucl. Instrum. Methods* **A 320**, 331 (1992).
- [15] F. Abe *et al.*, *Phys. Rev.* **D 54**, 6596 (1996).

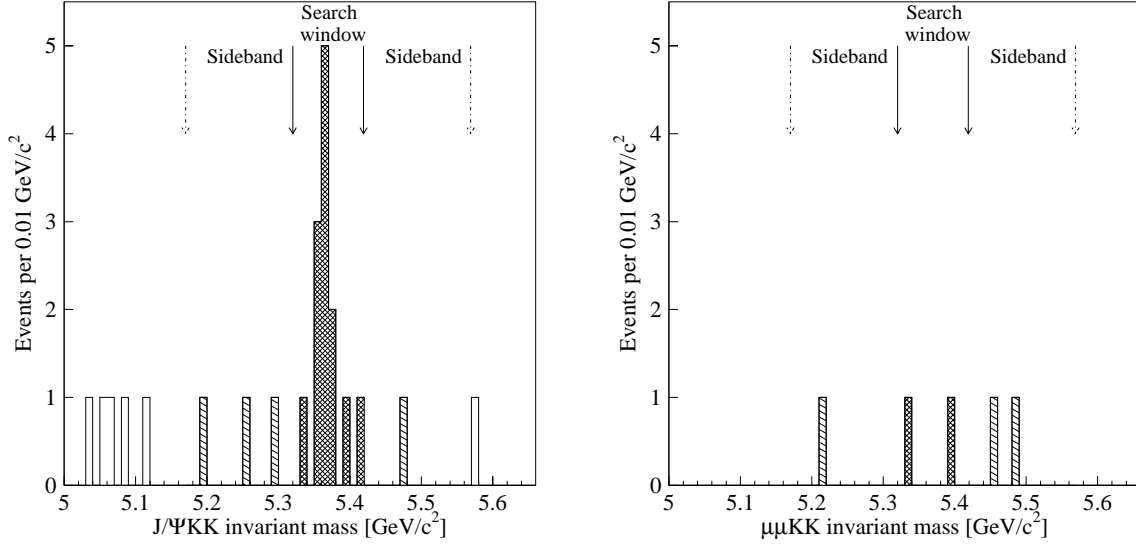


FIG. 1. Invariant mass distributions of $B_s \rightarrow J/\psi \phi$ (left) and $B_s \rightarrow \mu^+ \mu^- \phi$ (right) candidates after all selection requirements. The cross-hatched areas show the B_s signal region and the hatched areas the sideband regions.